

HSM2023-00046

ANALYSIS OF THE INCLINATION OF SLOTS IN TEXTURED CERAMIC TOOLS THROUGH THE STUDY OF THE FINAL ROUGHNESS AND CUTTING FORCES DURING CUTTING OF COLD WORK TOOL STEEL

P. Fernandez-Lucio^{1*}, O. Pereira², G. Urbikain¹, E. Ukar¹, L. N. Lopez de Lacalle²

¹University of the Basque Country (UPV/EHU), Department of Mechanical Engineering, Bilbao, Spain

²Aeronautics Advanced Manufacturing Centre (CAFA), University of the Basque Country (UPV/EHU), Zamudio, Spain

*Corresponding author; e-mail: pablo.fernandezd@ehu.eus

Abstract

This study investigates the influence of different texturing inclinations on the cutting forces and surface roughness during hard turning with ceramic cutting tools of X100CrMoV8 cold work tool steel. Four linear textures with inclinations ranging from 0° to 45° were tested. The results show that textured tools exhibited similar cutting forces to the reference tool, with a slight increase using a 30° inclination. Surface roughness measurements indicated minor variations among the textured tools, some reducing and others increasing roughness. The texturing inclinations had limited effects on cutting forces and surface roughness in this experimental setup.

Keywords:

Hard turning, Cold work tool steel, Ceramic tools, Textured tools, Laser engraving

1 INTRODUCTION

Hard turning is a technology that offers many advantages compared to grinding, commonly used for cutting hardened steels (45-65 HRC) such as bearing steels, cutting tools or moulds industry. First, hard turning offers greater flexibility in terms of component geometry. Moreover, it is faster than traditional grinding processes. In fact, hard turning improves the surface integrity of the component. Finally, it eliminates the use of harmful cooling [Tonshoff et al., 2000; Gaitonde et al., 2009 a].

In this process, large cutting forces are generated in addition to high temperatures in the contact area between tool and chip due to the high hardness of workpieces [Poulachon et al., 2001]. Therefore, for this process, tool materials are harder than the workpiece, such as CBN or ceramics [Bitterlich et al., 2008; Gaitonde et al., 2009 b].

Besides the higher hardness of the tool, the objective of using those kinds of tools is to make the tool work in adiabatic cutting. If that environment is achieved, most of the generated heat is evacuated with the chip, moving it away from the machined surface [Dudzinski et al., 2004; Bartarya et al., 2011].

The combination of large cutting forces, high workpiece hardness and high temperatures during cutting can damage the contact surfaces, decreasing the precision of the

component or modifying material properties. Hence, that challenging environment at the tool-workpiece interface on the rake face requires extreme characteristics of tool rigidity, tool toughness, and wear resistance. [Bouacha et al., 2014].

In cemented carbide cutting tools, chipbreakers minimise those harmful effects. Nonetheless, owing to temperature and pressure, manufacturing ceramic tools presents some technical problems in generating complex shapes on the rake face of ceramic inserts [Richards et al., 1989]. Thus, only simple geometries, such as buttons or square shapes, can be done.

Texturing techniques are a method to improve the performance and durability of cutting tools like ceramic ones thanks to enhance tribological behaviour during the cutting process. In fact, different researchers reduced the friction coefficient with textured tools [Orra et al., 2018; Ghosh et al., 2020]. Nevertheless, high temperatures generated during the cutting process can damage the surface quality and roughness of the machined component [Rajbongshi et al., 2018]. Hence, texturing inclinations can be used to reduce the impact of high cutting speeds on the part during machining, reducing the final roughness of the component [Li et al., 2019]. Moreover, by not using any coolant, the high cutting speeds achieved with ceramic

tools generate high cutting temperatures that can damage the surface roughness of the component and the tool itself. Regarding texturing in ceramic tools and their influence in the machining process, not much information has been found in the literature. Therefore, in order to reduce the impact of high cutting speeds on the component, this work analyses the influence of different texturing inclinations on the final roughness of the component and the cutting forces during cutting on Al₂O₃ with TiC for turning X100CrMoV8 cold work tool steel. For this purpose, four different linear textures will be tested by varying the inclinations of the grooves from 0° to 45° and compared with a reference tool without texture.

2 EXPERIMENTAL SETUP

CNGA 120408 inserts of alumina with titanium carbide (Al₂O₃ + TiC) were selected for the tests. The cutting edge presented a honed-chamfered edge with a chamfer of 200 μm with an inclination of 20° and a cutting edge radius of approximately 30 μm. The cutting conditions were based on manufacturer recommendations for roughing operations of cold work tool steels. In particular, a cutting speed of 180 m/min, feed of 0.15 mm/rev, and a depth of cut of 0.5 mm were used. The tests were carried out in dry conditions, as stated by the manufacturer of the tools. The toolholder used was DCLNR 2525M-12, which provides the cutting tool with a cutting edge angle of 95°, an orthogonal rake angle of -6°, and an inclination angle of -6°.

For the manufacture of the textures on the rake face of the tools, a Trumpf® Trumark 5000 station was used. This station is equipped with pulsed niobium: YAG fibre laser with an average output power of 50 W. The laser beam quality is characterised by an M² value of 1.6. The pulse frequency range goes from 1 to 1000 kHz with a minimum pulse duration of 7 nanoseconds. The laser spot size, when focused, has a 55 μm of diameter.

Fig. 1 shows the design of the textured tools tested in this study. Four different inclinations of grooves were tested, and their behaviours were compared with a tool without texturing used as a reference. Tab. 1 and Fig. 2 are shown the dimensional parameters of each tool. The inclination of the textured grooves is the unique dimensional parameter that was changed from one tool to another. The rest were designed the same. So as to respect the 200 μm chamfer, a space between the cutting edge and the start of the slots has been left. By reason of the laser used to manufacture the textures, slots had a parabolic shape with a depth of

approximately 9 μm. The programmed separation between grooves was 100 μm while the grooves' width was 75 μm.

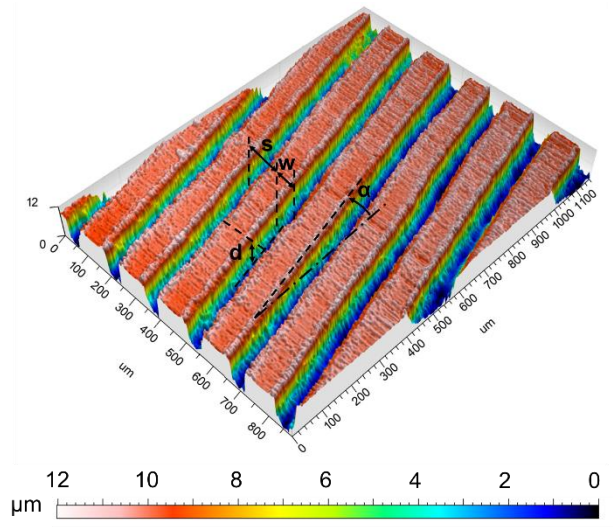


Fig. 2: Topography of the manufactured slots parameters.

Tab. 1: Grooves parameters.

Tool	s [μm]	w [μm]	d [μm]	α [°]
0°	94.0	63.2	9.0	0
15°	102.8	70.5	9.2	14.7
30°	107.5	74.0	9.4	29.6
45°	106.7	70.5	9.1	44.7

The chosen material for the validation of the proposed grooves was X100CrMoV8 steel. This kind of steel is a cold work tool commonly used for punching and cutting tools, plastic moulds, and pressure pads. Tab. 2 shows the main mechanical properties and the chemical composition of X100CrMoV8 steel.

Tests were carried out in a CMZ TC25BTY turning centre with 35 kW of power spindle and integral spindle. Cutting forces were registered with a triaxle Kistler® 9257B piezoelectric dynamometer and an OROS® OR35 real-time multi-analyser with a sampling frequency of 12,800 samples/s. The initial diameter of the workpiece was 86 mm, with a length of 350 mm. In Fig. 3, the experimental setup is presented. Only one pass was made with each tool to see the different textures' influence and avoid wear influence.

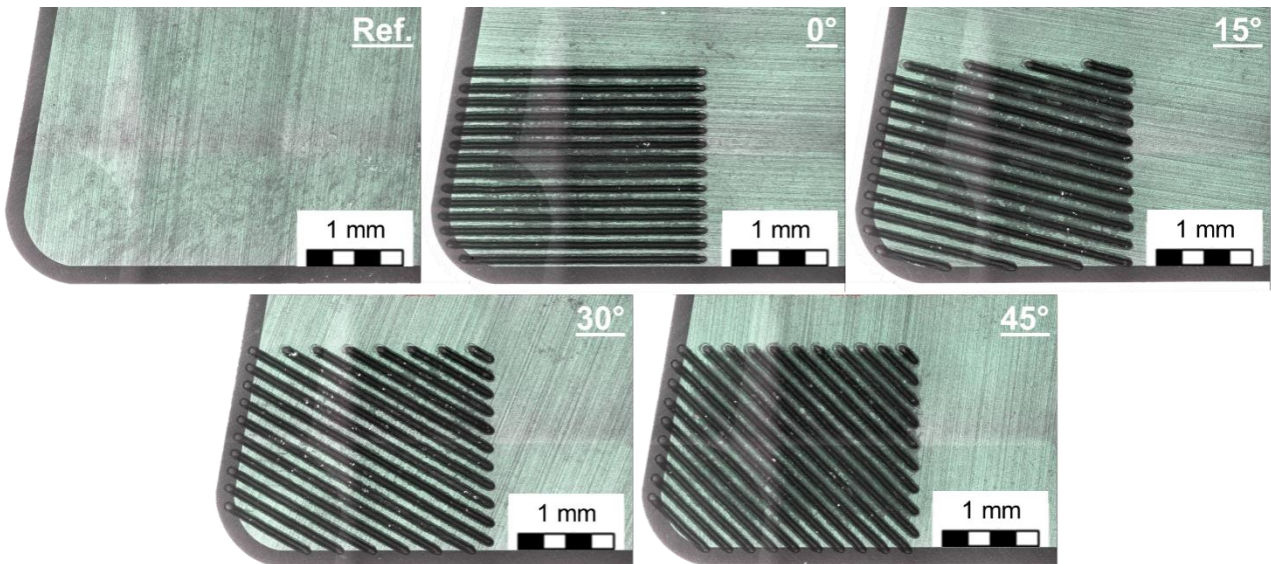


Fig. 1: Textured tools design. Tab. 2: Chemical composition and mechanical properties of tested X100CrMoV8 steel.

Chemical Composition (%)					
Fe	C	Cr	Mo	V	Si
Balance	1.0	8.0	1.1	1.6	0.9
Mechanical Properties					
Hardness	Young's Modulus	Tensile Strength	Density	Specific Heat	Thermal Conduct.
60 HRC	210 GPa	850 MPa	7940 kg/m ³	415 J/(kg·K)	24 W/(m·K)

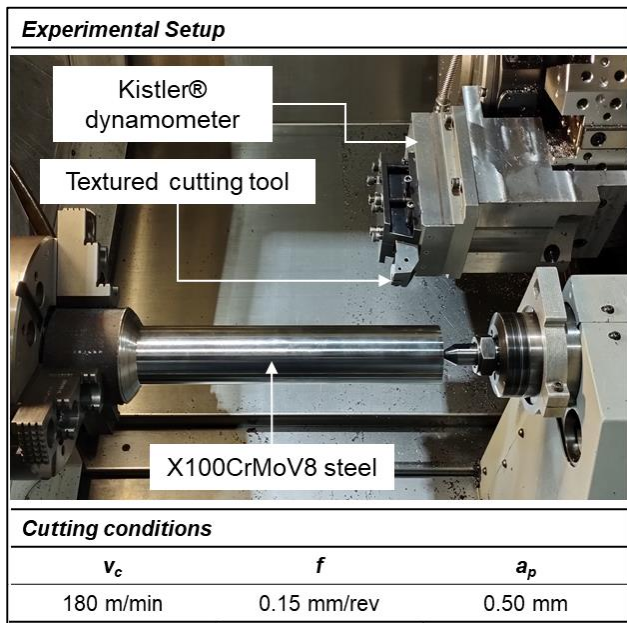


Fig. 3: Experimental setup.

3 RESULTS AND DISCUSSION

Fig. 4 are shown the rake faces of tested tools after machining. Despite the brittleness of ceramic tool material, it must be noticed that only a tiny crater can be seen on the tool's tip.

3.1 Cutting forces

In Fig. 5, the average of binormal force (F_b), tangential force or cutting force (F_c), feed force (F_f), and the calculated

modulus from the three force components in each test are shown. Binormal force is measured in the radial direction of the workpiece (red in Fig 5), cutting force in the tangential direction (green in Fig. 5), and feed force in the axial direction (blue in Fig. 5).

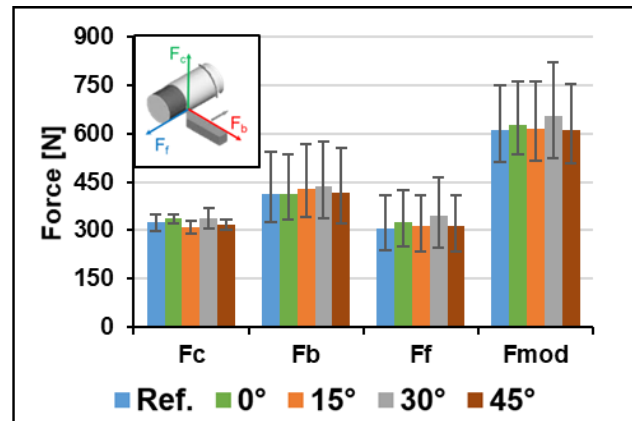


Fig. 5: Average cutting forces.

First, it should be noticed that the force with more significance was the binormal force (F_b), the force in the radial direction of the workpiece, which is in accordance with the studies carried out by [Yallese et al., 2009; Bartarya et al., 2011]. Two effects explain this behaviour: the hardness of the machined material and the geometry of the cutting itself as, during machining, a tooltip with a radius of 0.8 mm was being used, and the depth of cut was lower, 0.5 mm, than the tooltip. This behaviour is typical in machining with other cutting tool shapes, such as round inserts.

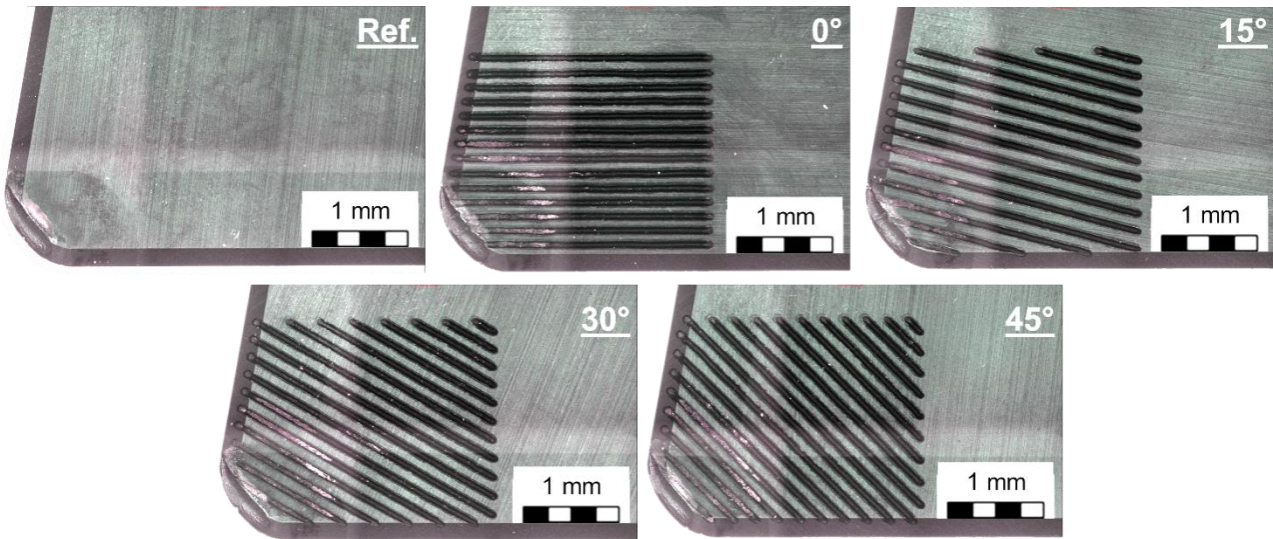


Fig. 4: Tools rake face after machining.

As can be seen in the figure, textured tools had similar average cutting forces. However, the most significant difference was with the 30° inclination, which increased a 7.1% the modulus of the resultant force. The other resultant forces were higher than the reference tool but below 3%, which leads to the conclusion that cutting forces are practically equal.

Nonetheless, it had been seen as a rare binormal and feed forces phenomenon. Fig. 6 is shown a scheme of forces performance. During machining, they significantly decreased, with a slope m_1 , until a point (point F_2 - v_2 in Fig. 6) when forces changed their slope to m_2 . At this point, the behaviour of each tested tool was different: some tools had a positive slope (F_{3a} in Fig. 6) while the others had a negative but not as much as before (F_{3b} in Fig. 6).

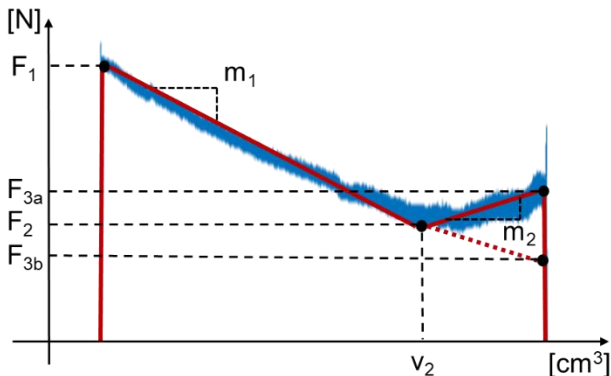


Fig. 6: Behaviour of binormal and feed force. In blue is the binormal force of the reference tool.

The point where forces changed was different for each cutting tool. The reference tool changed after 25.3 cm³ of machined material, which was the tool that took the longest to change. The other tools machined 20.4 cm³, 20.2 cm³, 22.3 cm³, and 21.5 cm³ of steel for 0°, 15°, 30°, and 45° inclinations respectively.

Tab. 3 is shown the values of F_1 , F_2 and F_3 for the binormal force of all the tested tools, whereas Fig. 7 is shown the two different slopes of each tool for the same force. Notice that slope is in N·cm⁻³, i.e., force divided by removed volume.

Tab. 3: Values of binormal force for slope changing points.

Tool	F_1 [N]	F_2 [N]	F_3 [N]
Ref.	532.8	251.5	263.8
0°	523.7	251.9	355.8
15°	551.9	381.4	363.5
30°	552.7	380.8	369.7
45°	542.6	351.5	341.6

Tool	F_1 [N]	F_2 [N]	F_3 [N]
Ref.	532.8	341.0	381.4
0°	523.7	351.9	355.8
15°	551.9	381.4	363.5
30°	552.7	380.8	369.7
45°	542.6	351.5	341.6

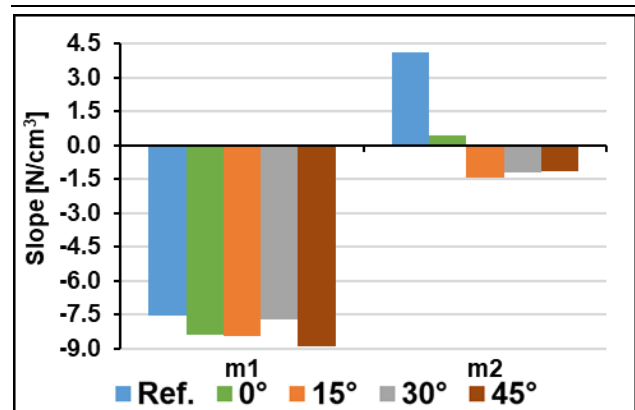


Fig. 7: Approximate slope values of binormal force.

It can be noticed that textured tools, except for 0° of inclination, had major force at the beginning of the cutting process. However, it presented the lower values at the point of changing slopes. Those lower values are explained due to the higher evacuated material up to that point. The tool with higher force at the intersection point was the 15° inclination tool, which also reached that point earlier. The other tools had similar behaviour in that first part.

Nevertheless, a big difference occurred after the transition point. The reference tool suffered a considerable increase in force, as seen by looking at the slope m_2 change in Fig. 7, which became positive. With the exception of the tool with 0° inclination that presented a low positive slope, textured tools continued with a negative trend but with lower values than before.

Tab. 4 is shown the values of F_1 , F_2 and F_3 for the feed force of all the tested tools, while Fig. 8 is shown the two different slopes of each tool for the same force.

Tab. 4: Values of feed force for slope changing points.

Tool	F_1 [N]	F_2 [N]	F_3 [N]
Ref.	395.3	251.5	263.8

0°	410.7	274.1	263.9
15°	397.9	281.1	246.8
30°	432.5	299.3	271.5
45°	399.6	266.0	245.3

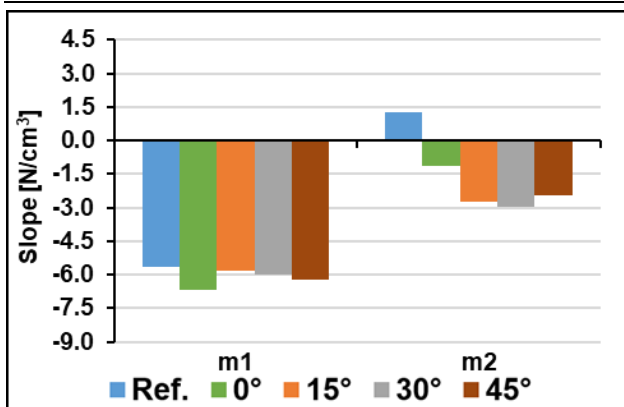


Fig. 8: Approximate slope values of feed force.

As occurred with the binormal force, the feed force initially decreased until a point. However, this force's slopes were

lower than in the previous case. As can be noticed, the first slope (m_1) was very similar for all the tested tools.

Once each force reached the transition point, all tested tools suffered a change. Although, in this case, that change was not as abrupt as with binormal force, i.e., for all tools, the second slope (m_2) was more similar to the first one. Moreover, in this case, the reference tool was the only one that presented a positive slope after the transition point.

This behaviour can be explained by the temperature generated during the cutting process, which softens the cut material until it stabilises and tool wear appears more dominant [Bartarya et al., 2011]. The steeper the slope, the greater the heat transfer.

3.2 Surface roughness

In terms of surface quality, all textured tools left a very similar machined surface, as can be seen in Fig. 9. According to literature, owing to texturing cutting tools, machined surface roughness can involve both a growth [Xing et al., 2014] and a decrease [Zhang et al., 2017]. Therefore, a deeper analysis of the surface roughness was carried out.

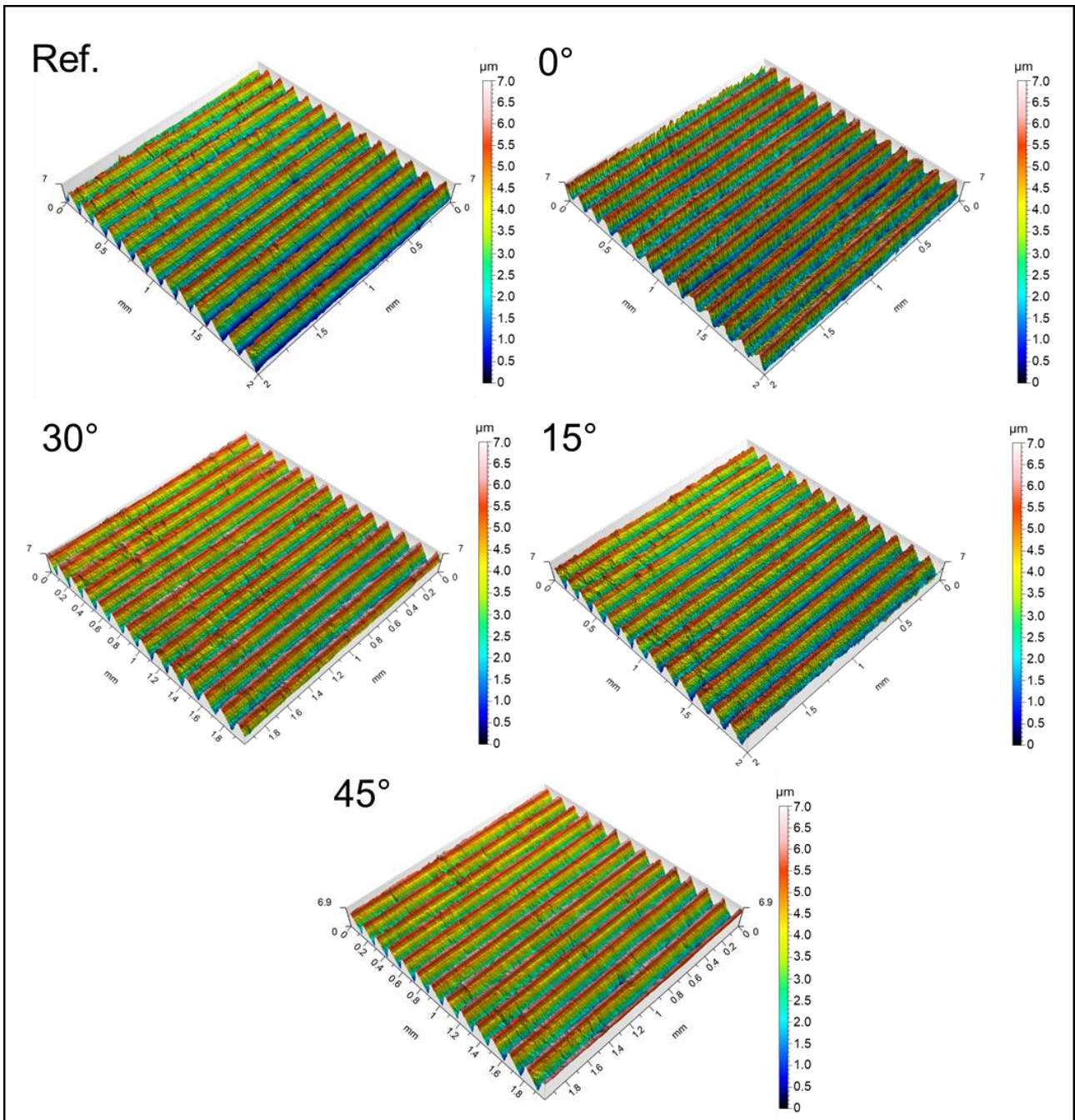


Fig. 9: Topographies of the machined surface with the different tested tools.

Fig. 10 and Fig. 11 show the average roughness (R_a and R_z , respectively) measurements, three for each tested tool, obtained in the machined surfaces. A cut-off length of 0.8 mm and an evaluation length of 4 mm were used for measuring settings according to standard ISO 4288: 1996 [Standard 1998].

As can be observed in the figure, some of the textured tools reduced surface roughness parameters, and others increased them, which is in accordance with the studies of Zhang et al. and Xing et al. [Xing et al., 2014; Zhang et al., 2017]. However, those differences were minimal.

In comparison with the reference tool, the R_a values of tools with 0° and 15° inclinations are enhanced (reduction of 1.7% and 5.1%, respectively), while values of tools with 30° and 45° increased roughness (an increase of 5.4% and 2.4%, respectively). Dispersions of R_a values obtained for all tested tools were very low.

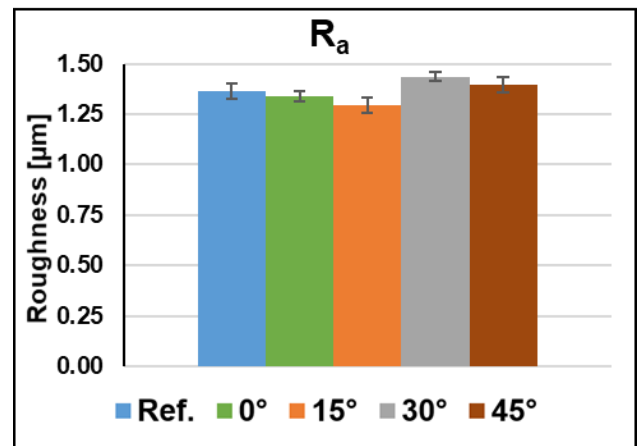


Fig. 10: Average roughness measurement R_a in the final machined surfaces.

This behaviour was different for the R_z values. In this case, all the tools presented lower roughness values than the reference tool. Those improvements were 6.4%, 7.7%, 3.7%, and 2.8% for 0°, 15°, 30°, and 45° inclinations respectively.

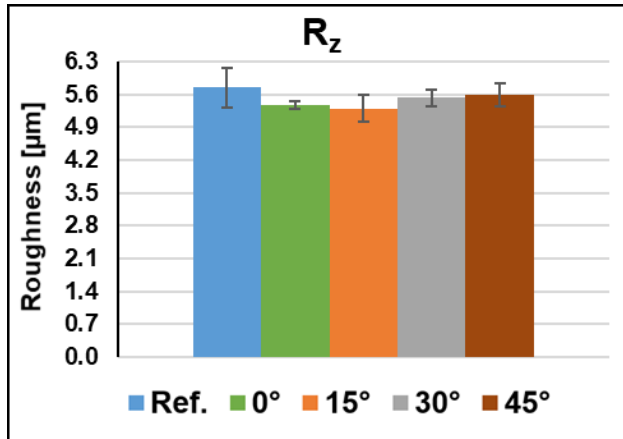


Fig. 11: Average roughness measurement R_z in the final machined surfaces.

4 CONCLUSIONS

This work analyses the influence of different texturing inclinations on the cutting forces t and the final roughness of the component during the cutting of Al_2O_3 with TiC for the turning of X100CrMoV8 cold work tool steel. The results showed that texturing inclinations could be used to mitigate the impact of high cutting speeds on the component during ceramic tool machining. After carrying out the tests and the different measurements, the following conclusions have been reached:

- Ceramic tools are a feasible solution for machining hard steels due to their excellent performance in high-temperature environments, improving cutting time productivity and tool life compared with cemented carbide tools.
- Cutting forces were very similar for all tested tools. The major difference with the reference tool was an increase of 7.1% with the 30° inclination textured tool. The rest tools presented equal forces with the reference one.
- All tested tools presented two different behaviours in the binormal and feed forces: first, a decrease and, then, the slope changes. That behaviour can be explained due to temperature increment during the cutting process until a point when tool wear starts to be dominant. This effect was higher with the reference tool.
- Regarding surface roughness, the 15° groove inclination optimises the reduction of R_a by 5.1% compared to the reference tool without texture and the R_z parameter by 7.7%.

5 ACKNOWLEDGMENTS

Authors are grateful to special Unit AIMS, funded by the University of the Basque Country, Ideko, IMH and BCAM, the Basque government project IT1337-19, the Spanish Ministry of PCD2021-121792-I00 and PID2019-109340RB-I00 projects and the UPV/EHU itself for the financial aid for the pre-doctoral grants PIF 19/96.

6 REFERENCES

- [Bartarya et al., 2011] Bartarya, G. and Choudhury, S. K., State of the art in hard turning. *International Journal of Machine Tools & Manufacture*, 2011, 53, 1–14.
- [Bitterlich et al., 2008] Bitterlich, B.; Bitsch, S. and Friederich, K., SiAlON based ceramic cutting tools. *Journal of the European Ceramic Society, Engineering {Ceramics}* '07: {From} {Engineering} {To} {Functionality}, 2008, 28, 989–994. ISSN 0955-2219.
- [Bouacha et al., 2014] Bouacha, K.; Yallese, M. A.; Khamel, S. and Belhadi, S., Analysis and optimisation of hard turning operation using cubic boron nitride tool. *International Journal of Refractory Metals and Hard Materials*, July 2014, 45, 160–178. ISSN 0263-4368.
- [Dudzinski et al., 2004] Dudzinski, D.; Devillez, A.; Moufki, A.; Larrouquère, D.; Zerrouki, V. and Vigneau, J., A review of developments towards dry and high speed machining of Inconel 718 alloy. *International Journal of Machine Tools and Manufacture*, March 2004, 44, 439–456. ISSN 08906955.
- [Gaitonde et al., 2009 a] Gaitonde, V. N.; Karnik, S. R.; Figueira, L. and Davim, J. P., Analysis of Machinability During Hard Turning of Cold Work Tool Steel (Type: AISI D2). *Materials and Manufacturing Processes*, December 2009a, 24, 1373–1382. ISSN 10426914.
- [Gaitonde et al., 2009 b] Gaitonde, V. N.; Karnik, S. R.; Figueira, L. and Paulo Davim, J., Machinability investigations in hard turning of AISI D2 cold work tool steel with conventional and wiper ceramic inserts. *International Journal of Refractory Metals and Hard Materials*, July 2009b, 27, 754–763. ISSN 0263-4368.
- [Ghosh et al., 2020] Ghosh, P. and Pacella, M., Effect of laser texturing on the performance of ultra-hard single-point cutting tools. *International Journal of Advanced Manufacturing Technology*, January 2020, 106, 2635–2648. ISSN 14333015.
- [Li et al., 2019] Li, Q.; Pan, C.; Jiao, Y. and Hu, K., Investigation on Cutting Performance of Micro-Textured Cutting Tools. *Micromachines* 2019, Vol. 10, Page 352, May 2019, 10, 352. ISSN 2072-666X.
- [Orra et al., 2018] Orra, K. and Choudhury, S. K., Tribological aspects of various geometrically shaped micro-textures on cutting insert to improve tool life in hard turning process. *Journal of Manufacturing Processes*, January 2018, 31, 502–513. ISSN 1526-6125.
- [Poulachon et al., 2001] Poulachon, G.; Moisan, A. and Jawahir, I. S., Tool-wear mechanisms in hard turning with polycrystalline cubic boron nitride tools. *Wear*, 2001, 250, 576–586.
- [Rajbongshi et al., 2018] Rajbongshi, S. K.; Annebushan Singh, M. and Kumar Sarma, D., A comparative study in machining of AISI D2 steel using textured and non-textured coated carbide tool at the flank face. *Journal of Manufacturing Processes*, December 2018, 36, 360–372. ISSN 1526-6125.
- [Richards et al., 1989] Richards, N. and Aspinwall, D., Use of ceramic tools for machining nickel based alloys. *International Journal of Machine Tools and Manufacture*, 1989, 29, 575–588. ISSN 08906955.
- [Standard, 1998] Standard, I., ISO - ISO 4288:1996/Cor 1:1998 - Geometrical Product Specifications (GPS) — Surface texture: Profile method — Rules and procedures for the assessment of surface texture — Technical Corrigendum 1, 1998, Retrieved from <https://www.iso.org/standard/29875.html>.

[Tonshoff et al., 2000] Tonshoff, H. K.; Arendt, C. and Amor, R. Ben, Cutting of Hardened Steel. *Annual CIRP*, 2000, 40, 547–466.

[Xing et al., 2014] Xing, Y.; Deng, J.; Zhao, J.; Zhang, G. and Zhang, K., Cutting performance and wear mechanism of nanoscale and microscale textured Al₂O₃/TiC ceramic tools in dry cutting of hardened steel. *International Journal of Refractory Metals and Hard Materials*, March 2014, 43, 46–58. ISSN 0263-4368.

[Yallese et al., 2009] Yallese, M. A.; Chaoui, K.; Zeghib, N.; Boulanouar, L. and Rigal, J. F., Hard machining of hardened bearing steel using cubic boron nitride tool. *Journal of Materials Processing Technology*, January 2009, 209, 1092–1104. ISSN 0924-0136.

[Zhang et al., 2017] Zhang, K.; Deng, J.; Ding, Z.; Guo, X. and Sun, L., Improving dry machining performance of TiAlN hard-coated tools through combined technology of femtosecond laser-textures and WS₂ soft-coatings. *Journal of Manufacturing Processes*, December 2017, 30, 492–501. ISSN 1526-6125.